

Analysis of Elliptic and Cylindrical striplines Using Laplace's Equation

K. K. JOSHI AND B. N. DAS

Abstract—Analysis of elliptic and cylindrical striplines based on Laplace's equation is presented. The solution of boundary value problem is obtained by an application of the modified residue calculus technique. The numerical results on the characteristic impedance are presented for a wide range of parameters. From the series solution of the Laplace's equation, the potential distribution is determined. The effect of warpage due to environmental changes on an otherwise planar structure is also estimated.

I. INTRODUCTION

THE PAPER presents an analysis of nonplanar striplines having elliptic and cylindrical configurations. Using the method of separation of variables, the solution of the two-dimensional Laplace's equation in orthogonal curvilinear elliptic coordinates is expressed in the form of a series which assumes different forms in different regions of the stripline. The constants appearing in the solution are determined by the modified residue calculus technique developed by Mittra [1]. The capacitance per unit length of the line and hence the characteristic impedance are determined by integrating the normal derivative of the potential function over the strip whose transverse section is a part of an ellipse. The potential distribution along the ellipse containing the strip is also determined.

The characteristic impedance for the cylindrical stripline can be determined from the above general formulation by treating it as a limiting case of an elliptic stripline. Numerical results for both the elliptic and cylindrical striplines are compared with those obtained by conformal mapping. The potential distribution along the circle passing through the circular arc-strip is determined. The effect of warpage on an otherwise planar structure is investigated. In the cases of both the cylindrical and cylindrically warped striplines, the results are compared with those obtained by Wang [2].

II. ELLIPTIC STRIPLINE

A cross section of an elliptic arc-strip placed between two confocal grounded elliptic cylinders is shown in Fig. 1(a). The two-dimensional potential function satisfies the

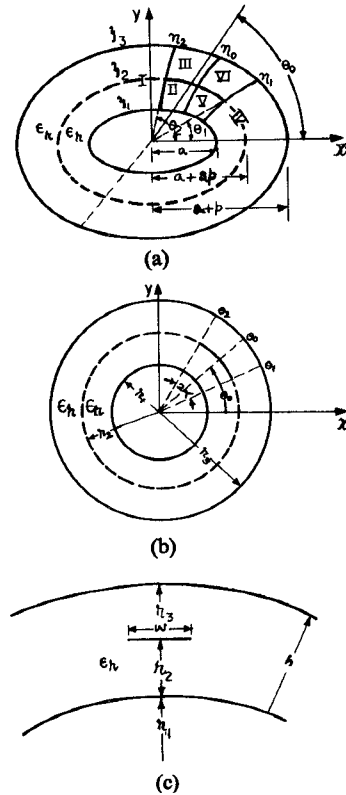


Fig. 1. Cross sections of (a) elliptic stripline; (b) cylindrical stripline; (c) warped stripline.

Laplace's equation [3]

$$\sqrt{\phi^2 - 1} \sqrt{1 - \psi^2} \left[\frac{\partial}{\partial \phi} \left(\sqrt{\frac{\phi^2 - 1}{1 - \psi^2}} \frac{\partial \psi}{\partial \phi} \right) + \frac{\partial}{\partial \psi} \left(\sqrt{\frac{1 - \psi^2}{\phi^2 - 1}} \frac{\partial \psi}{\partial \psi} \right) \right] = 0 \quad (1)$$

where ϕ and ψ are variables in orthogonal curvilinear coordinates. The curves $\phi = \text{constant}$ and $\psi = \text{constant}$, represent the sets of confocal ellipses and hyperbolas, respectively.

In order to solve (1), the change of variables

$$\begin{aligned} \phi &= \cosh \zeta \\ \psi &= \cos \eta \end{aligned} \quad (2)$$

is introduced.

Manuscript received June 11, 1979; revised November 5, 1979.

The authors are with the Department of Electronics and Electrical Communication Engineering, Indian Institute of Technology, Kharagpur 721302, India.

Using the method of separation of variables, the following equations are obtained from (1) and (2):

$$\begin{aligned} \frac{1}{F_1} \frac{d^2 F_1}{d\xi^2} &= -n^2 \\ \frac{1}{F_2} \frac{d^2 F_2}{d\eta^2} &= n^2 \end{aligned} \quad (3)$$

where n is a constant and $V = F_1(\xi)F_2(\eta)$. The solution of (3) is considered for the elliptic stripline, whose inner cylinder ($\xi = \xi_1 = \cosh^{-1} \phi_1$) has a semimajor axis of length a and the outer cylinder ($\xi = \xi_3 = \cosh^{-1} \phi_3$) has a semimajor axis of length equal to $a+p$. Further, the semimajor axis of an ellipse containing elliptic arc-strip ($\xi = \xi_2 = \cosh^{-1} \phi_2$) is assumed to be of length $a+sp$; where $0 < s < 1$. If the focal distance of these confocal elliptic cylinders from the origin of the coordinate system is k , it follows that

$$\begin{aligned} \xi_1 &= \cosh^{-1}(a/k) \\ \xi_2 &= \cosh^{-1}\left(\frac{a+sp}{k}\right) \\ \xi_3 &= \cosh^{-1}\left(\frac{a+p}{k}\right). \end{aligned} \quad (4)$$

The solutions for the potential function $V(\xi, \eta)$ in different regions of Fig. 1 (a) are obtained in Fourier series as follows:

region I:

$$V = \sum_{n=1}^{\infty} A_n \sin \alpha_n(\xi - \xi_1) e^{-\alpha_n(\eta - \eta_2)}, \quad \xi_1 < \xi < \xi_2, \eta_2 < \eta < \Pi + \eta_0 \quad (5)$$

$$V = \sum_{n=1}^{\infty} A_n \frac{\sin \alpha_n(\xi_2 - \xi_1)}{\sin \alpha_n(\xi_3 - \xi_2)} \sin \alpha_n(\xi_3 - \xi) e^{-\alpha_n(\eta - \eta_2)}, \quad \xi_2 < \xi < \xi_3, \eta_2 < \eta < \Pi + \eta_0 \quad (6)$$

region II:

$$V = \frac{V_0(\xi - \xi_1)}{(\xi_2 - \xi_1)} + \sum_{n=1}^{\infty} B_n \sin \beta_n(\xi - \xi_1) \cosh \beta_n(\eta - \eta_0), \quad \xi_1 < \xi < \xi_2, \eta_0 < \eta < \eta_2 \quad (7)$$

region III:

$$V = \frac{V_0(\xi_3 - \xi)}{(\xi_3 - \xi_2)} + \sum_{n=1}^{\infty} C_n \sin \gamma_n(\xi_3 - \xi) \cosh \gamma_n(\eta - \eta_0), \quad \xi_2 < \xi < \xi_3, \eta_0 < \eta < \eta_2 \quad (8)$$

region IV:

$$V = \sum_{n=1}^{\infty} D_n \sin \alpha_n(\xi - \xi_1) e^{-\alpha_n(\eta_1 - \eta)}, \quad \xi_1 < \xi < \xi_2, -\Pi + \eta_0 < \eta < \eta_1 \quad (9)$$

$$V = \sum_{n=1}^{\infty} D_n \frac{\sin \alpha_n(\xi_2 - \xi_1)}{\sin \alpha_n(\xi_3 - \xi_2)} \sin \alpha_n(\xi_3 - \xi) e^{-\alpha_n(\eta_1 - \eta)}, \quad \xi_2 < \xi < \xi_3, -\Pi + \eta_0 < \eta < \eta_1 \quad (10)$$

region V:

$$V = \frac{V_0(\xi - \xi_1)}{(\xi_2 - \xi_1)} + \sum_{n=1}^{\infty} E_n \sin \beta_n(\xi - \xi_1) \cosh \beta_n(\eta_0 - \eta), \quad \xi_1 < \xi < \xi_2, \eta_1 < \eta < \eta_0 \quad (11)$$

region VI:

$$V = \frac{V_0(\xi_3 - \xi)}{(\xi_3 - \xi_2)} + \sum_{n=1}^{\infty} F_n \sin \gamma_n(\xi_3 - \xi) \cosh \gamma_n(\eta_0 - \eta), \quad \xi_2 < \xi < \xi_3, \eta_1 < \eta < \eta_0 \quad (12)$$

where

$$\begin{aligned} \alpha_n &= n\Pi/(\xi_3 - \xi_1) \\ \beta_n &= n\Pi/(\xi_2 - \xi_1) \\ \gamma_n &= n\Pi/(\xi_3 - \xi_2). \end{aligned} \quad (13)$$

In the particular case of $\eta_2 = 2\eta_0 - \eta_1$, the solutions for the regions I-III and IV-VI become identical and further analysis may be carried out by considering (5)-(8) only. The above potential functions satisfy the boundary conditions $V = V_0$ on the elliptic arc-strip and $V = 0$ on the grounded elliptic cylinders. Use of the continuity of the potential function V and its normal derivative at the interface $\eta = \eta_2$ and the orthogonality of the functions $\sin \beta_n(\xi - \xi_1)$ and $\sin \gamma_n(\xi_3 - \xi)$ over the intervals of ξ_1 to ξ_2 and ξ_2 to ξ_3 , respectively, elimination of the constants B_m and C_m appearing in (7)-(8) leads to the following equations [1]:

$$\sum_{n=1}^{\infty} \frac{\bar{A}_n}{\alpha_n - \beta_m} + \lambda_m \sum_{n=1}^{\infty} \frac{\bar{A}_n}{\alpha_n + \beta_m} = \frac{1}{-\beta_m} + \frac{\lambda_m}{\beta_m} \quad (14)$$

$$\sum_{n=1}^{\infty} \frac{\bar{A}_n}{\alpha_n - \gamma_m} + \xi_m \sum_{n=1}^{\infty} \frac{\bar{A}_n}{\alpha_n + \gamma_m} = \frac{1}{-\gamma_m} + \frac{\xi_m}{\gamma_m} \quad m = 1, 2, \dots \quad (15)$$

where

$$\lambda_m = \exp[-2\beta_m(\eta_2 - \eta_0)] \quad (16)$$

$$\xi_m = \exp[-2\gamma_m(\eta_2 - \eta_0)] \quad (17)$$

$$\bar{A}_n = A_n \sin \alpha_n(\xi_2 - \xi_1)$$

and

$$V_0 = 1.$$

Solution of the above set of equations can be obtained from the meromorphic function $f(w)$ of the complex variable w , which has the following properties [1].

1) $f(w)$ has simple poles at $w = \alpha_n$, $n = 1, 2, \dots$ and at $w = 0$.

2)

$$f(\beta_m) + \lambda_m f(-\beta_m) = 0$$

$$f(\gamma_m) + \xi_m f(-\gamma_m) = 0, \quad m = 1, 2, \dots$$

3) $f(w)$ has the asymptotic behavior $f(w) \sim K_1 |w|^{-\nu}$ as $|w| \rightarrow \infty$, $K_1 = \text{constant}$, $1 < \nu < 2$.

4) The residue of $f(w)$ at $w = 0$, say $R_f(0)$, is -1 . The

function $f(w)$ may be expressed as

$$f(w) = Kg(w) P(w) \quad (18)$$

where

$$g(w) = e^{Rw} \frac{\Pi(w, \beta_n) \Pi(w, \gamma_n)}{w \Pi(w, \alpha_n)}$$

$$R = \frac{1}{\Pi} \left[(\xi_2 - \xi_1) \ln \left(\frac{\xi_3 - \xi_1}{\xi_2 - \xi_1} \right) + (\xi_3 - \xi_2) \ln \left(\frac{\xi_3 - \xi_1}{\xi_3 - \xi_2} \right) \right]$$

$$\Pi(w, \alpha_n) = \prod_{n=1}^{\infty} \left(1 - \frac{w}{\alpha_n} \right) e^{w(\xi_3 - \xi_1)/n\Pi}$$

$$\Pi(w, \beta_n) = \prod_{n=1}^{\infty} \left(1 - \frac{w}{\beta_n} \right) e^{w(\xi_2 - \xi_1)/n\Pi}$$

$$\Pi(w, \gamma_n) = \prod_{n=1}^{\infty} \left(1 - \frac{w}{\gamma_n} \right) e^{w(\xi_3 - \xi_2)/n\Pi}$$

and

$$P(w) = 1 + \sum_{m=1}^{\infty} \frac{F_m}{1 - (w/\beta_m)} + \sum_{m=1}^{\infty} \frac{G_m}{1 - (w/\gamma_m)}. \quad (19)$$

The constants K, F_m , and G_m appearing in (18) and (19) are evaluated from the properties 2)–4) of $f(w)$ described above. Since F_m and G_m are rapidly convergent, the construction of the meromorphic function $f(w)$ involves inversion of a small size matrix [1]. Following the procedure suggested by Mittra [1], the constants A_n, B_m , and C_m are obtained as

$$A_n \sin [\alpha_n(\xi_2 - \xi_1)] = R_f(\alpha_n) = D_n \sin [\alpha_n(\xi_2 - \xi_1)] \quad (20a)$$

$$F_m = B_m = (-1)^m \frac{2}{(\xi_2 - \xi_1)} f(-\beta_m) \exp [-\beta_m(\eta_2 - \eta_0)] \quad (20b)$$

$$E_m = C_m = (-1)^m \frac{2}{(\xi_3 - \xi_2)} f(-\gamma_m) \exp [-\gamma_m(\eta_2 - \eta_0)]. \quad (20c)$$

In (20a), $R_f(\alpha_n)$ is the residue of $f(w)$ at $w = \alpha_n$. Substituting (20) in (5)–(8) for the potential function and taking its normal derivative on the elliptic arc-strip ($\xi = \xi_2$), the expression for the charge distribution on the elliptic arc-strip is obtained as

$$\begin{aligned} \frac{\rho_1(\eta)}{\epsilon_r \epsilon_0} &= \frac{1}{\xi_2 - \xi_1} + \frac{1}{\xi_3 - \xi_2} \\ &+ \sum_{m=1}^{\infty} \frac{m\Pi}{(\xi_2 - \xi_1)^2} f(-\beta_m) [e^{-\beta_m(\eta_2 - \eta)} + e^{-\beta_m(\eta - 2\eta_0 + \eta_2)}] \\ &+ \sum_{m=1}^{\infty} \frac{m\Pi}{(\xi_3 - \xi_2)^2} f(-\gamma_m) [e^{-\gamma_m(\eta_2 - \eta)} + e^{-\gamma_m(\eta - 2\eta_0 + \eta_2)}], \end{aligned} \quad (21)$$

$$\eta_0 < \eta < \eta_2. \quad (21)$$

Making use of the asymptotic form of $f(w)$ for large values of w , it may be shown that the summation appear-

ing in the expression for the charge distribution, in the neighborhood of $\eta \rightarrow \eta_2$ reduces to the form [1]

$$\sum_{m=1}^{\infty} m^{-1/2} e^{-m\Pi(\eta_2 - \eta)/(\xi_2 - \xi_1)} \sim \left[\frac{1}{(\xi_2 - \xi_1)} (\eta_2 - \eta) \right]^{-1/2} \quad (22)$$

and the charge distribution on the strip in the neighborhood of $\eta \rightarrow \eta_2$ assumes the form:

$$\begin{aligned} \frac{\rho_2(\eta)}{\epsilon_r \epsilon_0} &= \frac{1}{\xi_2 - \xi_1} + \frac{1}{\xi_3 - \xi_2} + \frac{2K}{\sqrt{\Pi}} (\eta_2 - \eta)^{-1/2} \\ &+ \frac{2K}{\sqrt{\Pi}} (\eta_2 - 2\eta_0 + \eta)^{-1/2}. \end{aligned} \quad (23)$$

For various combinations of p/a ratio, S , and k , the values of $\eta = \eta_2 - \Delta$, which satisfy (22), are determined. Integrating (21) from η_0 to $\eta_2 - \Delta$ and (23) from $(\eta_2 - \Delta)$ to η_2 with respect to η the expression for the total charge on the strip, in view of the relation $\eta_2 - \eta_0 = \eta_0 - \eta_1$, is obtained as

$$Q = 2(Q_1 + Q_2) \quad (24a)$$

where

$$Q_1 = \int_{\eta_0}^{\eta_2 - \Delta} \rho_1(\eta) d\eta \quad (24b)$$

$$Q_2 = \int_{\eta_2 - \Delta}^{\eta_2} \rho_2(\eta) d\eta. \quad (24c)$$

Since it has been assumed that $V_0 = 1$, the capacitance of the structure is given by

$$C = 2(Q_1 + Q_2) \quad (25)$$

and the impedance is given by

$$\sqrt{\epsilon_r} Z_0 = \frac{120\Pi}{(C/\epsilon_r \epsilon_0)}. \quad (26)$$

The evaluation of the characteristic impedance of the strip involves construction of $P(w)$, satisfying (2). In actual computation the infinite product has to be truncated. The estimated error in the truncated product has been found to be quite small [1]. The unknown coefficients F_m and G_m appearing in expression of $P(w)$ have an exponential decay with the index m . Thus the determination of only a few of these lead to a fairly accurate solution of the problem under investigation [1].

Using expressions (4), (13), (16)–(19) and satisfying condition (2), F_m and G_m required for the construction of $f(w)$ are evaluated for values of $(\eta_2 - \eta_1)$ ranging from 1.5° to 120° for the following cases.

- 1) $p/a = 0.1, s = 0.3$, and $k/a = 0.25, 0.5$, and 0.75 .
- 2) $p/a = 0.25, s = 0.3$, and $k/a = 0.25, 0.5$, and 0.75 .
- 3) $p/a = 0.5, s = 0.3$, and $k/a = 0.25, 0.5$, and 0.75 .
- 4) $p/a = 1.0, s = 0.3$, and $k/a = 0.25, 0.5$, and 0.75 .
- 5) $p/a = 1.5, s = 0.3$, and $k/a = 0.8$.

The variation of the characteristic impedance with $\eta_2 - \eta_1$ is evaluated from (21)–(26) and the results are presented in Fig. 2. For the sake of comparison the results on characteristic impedance obtained by conformal mapping

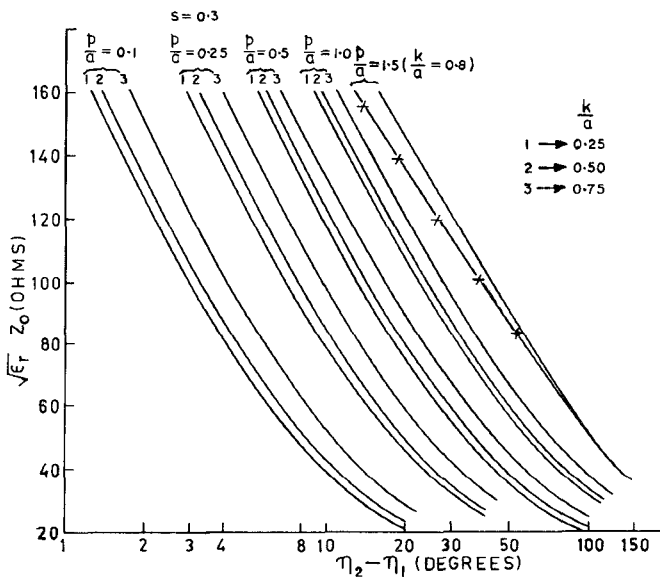


Fig. 2. Variation of the characteristic impedance for the elliptic stripline; $s=0.3$ (— = present method, -x-x- = conformal mapping).

are also presented in the same figure for $p/a = 1.5$, $s = 0.3$, and $k/a = 0.8$. Using the successive transformations [4], [5], an elliptic stripline can be transformed into a parallel plate configuration from which the characteristic impedance is evaluated.

The variation of the characteristic impedance with $\eta_2 - \eta_1$ for $S = 0.5$ and 0.7 and various values of p/a and k/a are presented in Figs. 3 and 4, respectively.

The variable $\eta_2 - \eta_1$ can be expressed in terms of θ_2 and θ_1 , the angles made by the edges of the elliptic strip with the major axis of the ellipse. The relationship is given by

$$\eta_2 - \eta_1 = \tan^{-1} \left[\frac{\coth \xi_2 (\tan \theta_2 - \tan \theta_1)}{1 + \coth^2 \xi_2 \tan \theta_2 \tan \theta_1} \right].$$

If $\theta_2 = \theta_0 + \Delta\theta$ and $\theta_1 = \theta_0 - \Delta\theta$, then

$$\eta_2 - \eta_1 = \tan^{-1} \frac{\coth \xi_2 [\tan (\theta_0 + \Delta\theta) - \tan (\theta_0 - \Delta\theta)]}{1 + \coth^2 \xi_2 \tan (\theta_0 + \Delta\theta) \tan (\theta_0 - \Delta\theta)}. \quad (27)$$

From (27) it is evident that the characteristic impedance depends on θ_0 , $\Delta\theta$ and also on ξ_2 which is related to the eccentricity k/a . From the results shown in Figs. 2-4 and (27), the dependence of the characteristic impedance on θ_0 and $\Delta\theta$ can be determined. Expression (27) reveals that for large ξ_2 (corresponding to small values of eccentricity k/a), $\coth \xi_2$ approaches unity and $\eta_2 - \eta_1$ approximates $2\Delta\theta$. For such cases, the characteristic impedance is practically independent of θ_0 . For lower values of ξ_2 corresponding to higher values of k/a , dependence of the characteristic impedance on θ_0 is of significance. For a particular value of eccentricity and θ_0 , the impedance decreases with increase in $\Delta\theta$. Further, for a particular $\Delta\theta$ and eccentricity, the impedance increases as θ_0 increases from 0° to 90° . The curves of Figs. 2-4 can be used to

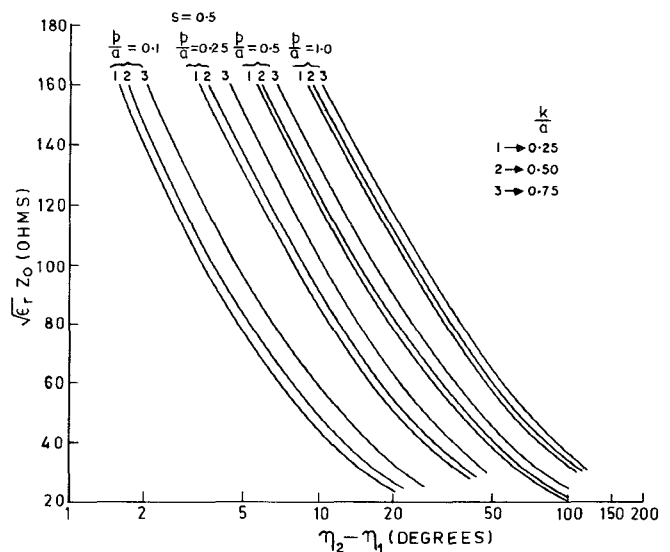


Fig. 3. Variation of the characteristic impedance for the elliptic stripline; $s=0.5$.

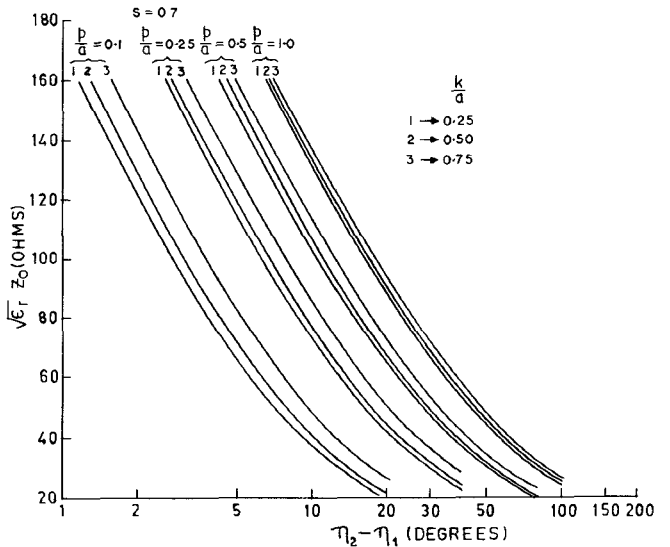


Fig. 4. Variation of the characteristic impedance for the elliptic stripline; $s=0.7$.

determine the characteristic impedance for a number of combinations of eccentricity k/a , θ_0 , and $\Delta\theta$.

Using the results of F_m and G_m obtained for $p/a = 1.5$, $k/a = 0.8$, and $s = 0.3$, $\eta_2 - \eta_0 = 23^\circ$ and evaluating the residue of $f(w)$ at $w = \alpha_n$, the potential function at $\xi = \xi_2$ for $\eta_2 < \eta < \Pi + \eta_0$ is calculated from

$$V(\xi_2, \eta) = \sum_{n=1}^{\infty} R_f(\alpha_n) e^{-\alpha_n(\eta - \eta_2)}. \quad (28)$$

The variation of the potential $V(\xi_2, \eta)$ for the above case is presented in Fig. 5(a).

III. CYLINDRICAL AND WARPED STRIPLINE

The cross section of a cylindrical stripline consisting of a circular arc-strip at a potential V_0 , placed between two

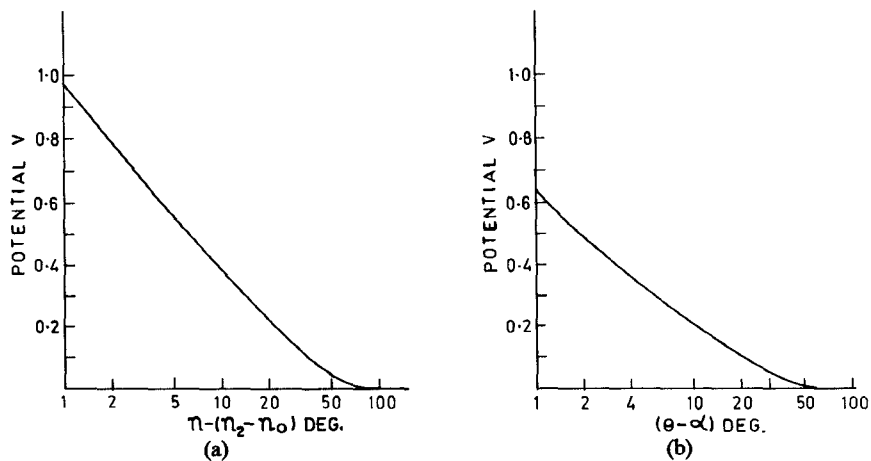


Fig. 5. (a) Potential distribution along the ellipse ($\xi = \xi_2$) for $\eta_2 < \eta < \Pi + \eta_0$, $p/a = 1.5$, $s = 0.3$, $k/a = 0.8$, and $\eta_2 - \eta_0 = 23^\circ$. (b) Potential distribution along the circle ($r = a + sp$) for $\theta_2 < \theta < \Pi + \theta_0$, $p/a = 1$, $s = 0.4$, and $\alpha = 30^\circ$.

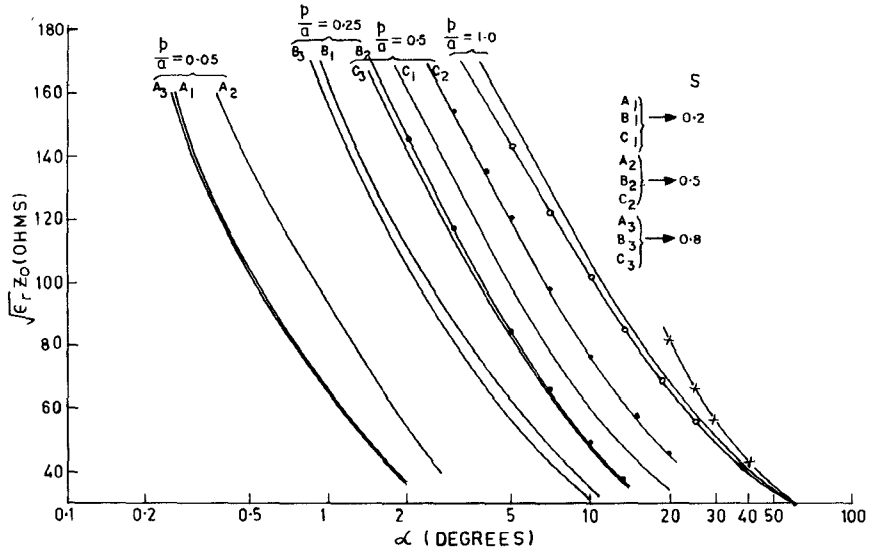


Fig. 6. Variation of the characteristic impedance of cylindrical stripline with strip half-angle; (— = present method, -0-0- = conformal mapping method, -x-x- = Wang's method [2].)

grounded concentric cylinders is shown in Fig. 1(b). Radii of the inner and outer cylinders are $r_1 (= a)$ and $r_2 (= a + p)$, respectively, and that of the arc-strip is $r_2 (= a + sp)$. The cylindrical stripline can be considered as a limiting case of an elliptic stripline. As $k \rightarrow 0$, the ellipses and hyperbolas degenerate into circles and radial lines, respectively. From (4), it is found that for $k=0$,

$$\begin{aligned}\xi_3 - \xi_1 &= \ln \left(\frac{a+p}{a} \right) \\ \xi_2 - \xi_1 &= \ln \left(\frac{a+sp}{a} \right) \\ \xi_3 - \xi_2 &= \ln \left(\frac{a+p}{a+sp} \right)\end{aligned}\quad (29)$$

and

$$\begin{aligned}\eta_1 &= \theta_1 \\ \eta_2 &= \theta_2 \\ \eta_0 &= \theta_0.\end{aligned}\quad (30)$$

The angle 2α , subtended by the arc-strip at the center is given by

$$2\alpha = \theta_2 - \theta_1 = 2(\theta_0 - \theta_1). \quad (31)$$

Substituting (29)–(31) in (4)–(26) and following the procedure described in Section II, the variation of the characteristic impedance as a function of the strip half-angle is determined for various values of p/a and s . The results are presented in Fig. 6. In the same figure the impedance obtained by conformal mapping for $p/a = 1$, $s = 0.4$ is shown for the sake of comparison. It may be pointed out that Wang [2] determined the characteristic impedance of the cylindrical stripline for the same values of parameters and the strip half-angles greater than 20° . These results are also presented in Fig. 6.

For the particular case of strip radius equal to the geometric mean of the radii of the two outer cylinders, the variation of the characteristic impedance as a function of

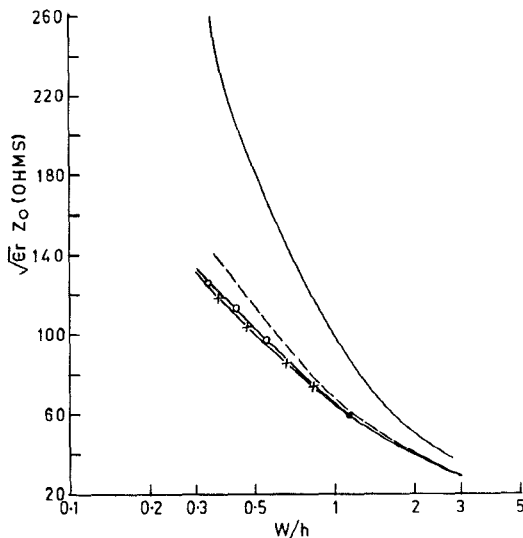


Fig. 7. Variation of the characteristic impedance as a function of width-to-height ratio w/h of a warped stripline; $h/a=0.01$, $s=0.5$ (--- = present method, -0-0 = planar symmetric formulation [6], -x-x = conformal mapping method, — Wang's method [2]).

the strip half-angle is shown by the dots in the same figure for $s=0.5$, $p/a=0.25$, and 0.5 . It is evident that if the strip radius is the geometric mean of the radii of the two outer cylinders, the characteristic impedance is maximum.

Following the procedure described in Section II, the potential distribution at the radius of $r=a+sp$, for $\theta_2 < \theta < \pi + \theta_0$ is calculated for $p/a=1$, $s=0.4$, and $\alpha=30^\circ$. The results are presented in Fig. 5(b).

In order to study the effect of warpage on an otherwise planar stripline, a symmetrical structure with $r_2-r_1=r_3-r_2=h/2$, where $h=r_3-r_1$, is considered. For an arc-strip of length W subtending an angle 2α at the center, $W=2\alpha r_2$. A warped structure shown in Fig. 1(c) can be obtained for small angle and large radius. The warpage of the line is indicated by the height to radius ratio h/a .

Using (13), (16)–(19), and (21)–(26), the variation of the characteristic impedance as a function of the width-to-

height ratio w/h of the strip is evaluated for $h/a=0.01$ and $s=0.5$, the results are presented in Fig. 7 together with those obtained by conformal mapping technique and also by Wang [2] using numerical solution of Laplace's equation. In the same figure, the numerical results obtained by Mittra [6] for an almost symmetric planar stripline ($s=1/\sqrt{3.999}$) are also presented for the sake of comparison. It is found that the results obtained by Wang [2] show a marked deviation from those obtained by other methods.

CONCLUSION

The numerical results for the characteristic impedance obtained by the application of the modified residue calculus technique do not exhibit marked deviation from those obtained by conformal mapping technique for both the elliptic and cylindrical striplines. For large strip angles the hyperbolic functions appearing in (5)–(8) can be approximated by exponential functions. The characteristic impedance in this case can be determined from purely analytical solution of Laplace's equation. For the case of the cylindrical and cylindrically warped striplines, the results obtained by the present method are found to be close to those obtained by conformal mapping. The results obtained by Wang [2] show an appreciable deviation for low strip angles.

REFERENCES

- [1] R. Mittra, *Computer Techniques for Electromagnetics*. New York: Pergamon, 1973, ch. 6, pp. 306–315.
- [2] Y. C. Wang, "Cylindrical and cylindrically warped strip and microstrip lines," *IEEE Trans. Microwave Theory Tech.*, vol. MTT-26, pp. 20–23, Jan. 1978.
- [3] J. A. Stratton, *Electromagnetic Theory*. New York: McGraw-Hill, 1941, p. 50, 200.
- [4] L. A. Pipes, *Applied Mathematics for Engineers and Physicists*. New York: McGraw-Hill, ch. XX, pp. 489–491.
- [5] J. S. Rao and B. N. Das, "Analysis of asymmetric stripline by conformal mapping," *IEEE Trans. Microwave Theory Tech.*, vol. MTT-27, pp. 299–303, Apr. 1979.
- [6] R. Mittra and T. Itoh, "Charge and potential distributions in shielded striplines," *IEEE Trans. Microwave Theory Tech.*, vol. MTT-18, pp. 149–156, Mar. 1970.